Article:
Barducci, L, Pittiglio, G, Norton, JC et al. (2019) Adaptive Dynamic Control for Magnetically Actuated Medical Robots. IEEE Robotics and Automation Letters, 4 (4). pp. 3633-3640. ISSN: 2377-3766

https://doi.org/10.1109/LRA.2019.2928761

Adaptive Dynamic Control for Magnetically Actuated Medical Robots

Lavinia Barducci[1], Giovanni Pittiglio[1], Joseph C. Norton[1], Keith L. Obstein[2], and Pietro Valdastri[1]

***Abstract*—In the present work we discuss a novel dynamic control approach for magnetically actuated robots, by proposing an *adaptive control* technique, robust towards parametric uncertainties and unknown bounded disturbances. The former generally arise due to partial knowledge of the robots' dynamic parameters, such as inertial factors, the latter are the outcome of unpredictable interaction with unstructured environments. In order to show the application of the proposed approach, we consider controlling the Magnetic Flexible Endoscope (MFE) which is composed of a soft-tethered Internal Permanent Magnet (IPM), actuated with a single External Permanent Magnet (EPM). We provide with experimental analysis to show the possibility of levitating the MFE - one of the most difficult tasks with this platform - in case of partial knowledge of the IPM's dynamics and no knowledge of the tether's behaviour. Experiments in an acrylic tube show a reduction of contact of the 32% compared to non-levitating techniques and 1.75 times faster task completion with respect to previously proposed levitating techniques. More realistic experiments, performed in a colon phantom, show that levitating the capsule achieves faster and smoother exploration and that the minimum time for completing the task is attained by the proposed approach.**

***Index Terms*—Magnetic Robots Control, Dynamic Control, Capsule Colonoscopy.**

I. Introduction

MAGNETICALLY actuated robots have been investigated during the last decades, particularly in the field of medical robotics. The main advantage of magnetically actuated robots is the potential miniaturization; this approach permits to overcome complex and bulky actuation system, achieving *minimally invasiveness*. This is generally equated to a reduction of patient discomfort and post-operative recovery time. Miniaturization is also feasible because functional forces can be maintained by balancing an arbitrarily small Internal Permanent Magnets (IPMs) with a sufficiently large External Permanent Magnet (EPM).

Due to these advantages, this class of robot has been investigated for application to several fields of medicine, from endoscopic procedures, such as *colonoscopy* [1], [2], [3], *gastroscopy* [4] and *cardiac applications* [5], [6], [7], [8], [9] to *microrobotics* [10]. Magnetic external actuation can vary from coil-based systems [11], [5], [12], [13], [14], [15], [16], rotating permanent magnet-based devices [17], [18] and permanent magnet-based systems [1], [2], [3], [4], [19]. All these actuation mechanisms share similar control properties, in fact, actuation is based on employing the previously mentioned actuators for generating forces and torques focused on magnetic agents. Since the control inputs for these robots are forces and torques, it is particularly effecacious to consider a quasi-static [11], [12] or a dynamic control approach [20]. The latter has the advantage of considering the overall physical properties of the robots and permits faster and more accurate control.

We propose an *adaptive dynamic control* approach [21], able to cope with parametric uncertainties, such as inertial factors, and robust towards the presence of unknown bounded external disturbances. The former are, generally, related to partial knowledge of the robots' mechanical properties, the latter may be related to unstructured forces arising from the interaction with an unknown environment. This control technique employs the knowledge of the IPM pose, achieved by using an appropriate localization technique such as [22] or [23].

In order to discuss the application of the proposed technique, we focus on the control of the Magnetic Flexible Endoscope (MFE) [1], a innovative minimally invasive platform for colonoscopy. We consider the case of actuating a single *soft-tethered* IPM by employing a robotically manipulated EPM. Moreover, we consider partial knowledge of the mass and dimensions of the IPM and no information about the tether. While we focus on one platform, this proposed method could be applied to other actuation systems and untethered capsules [17].

Herein, we show successful *magnetic levitation* [20] which helps overcoming the major issue of previously proposed control techniques [24]: continuous attraction between the IPM and EPM. Successful levitation can encourage obstacle avoidance and a smoother navigation. It can also result in a reduction of pressure applied to the environment which will

Manuscript received: February, 22, 2019; Revised May, 29, 2019; Accepted July, 1, 2019.

This paper was recommended for publication by Editor P. Rocco upon evaluation of the Associate Editor and Reviewers' comments.

This research was supported by the Royal Society, UK, by the Engineering and Physical Sciences Research Council, UK under grant number EP/P027938/1 and EP/K034537/1, and by the National Institute of Biomedical Imaging and Bioengineering, USA of the National Institutes of Health under award no. R01EB018992. Any opinions, findings, conclusions, or recommendations expressed in this material are those of the authors and do not necessarily reflect the views of the Royal Society, the Engineering and Physical Sciences Research Council, or the National Institutes of Health.

L. Barducci and G. Pittiglio contributed equally to this work.

[1]L. Barducci, G. Pittiglio, J. C. Norton and P. Valdastri are with the STORM Lab UK, Institute of Robotics, Autonomous Systems and Sensing, School of Electronic and Electrical Engineering, University of Leeds, Leeds, UK {ellb, g.pittiglio, j.c.norton, p.valdastri}@leeds.ac.uk

[2]K. L. Obstein is with the Division of Gastroenterology, Hepatology, and Nutrition, Vanderbilt University Medical Center, Nashville, TN, USA, and with the STORM Lab, Department of Mechanical Engineering, Vanderbilt University, Nashville, TN, USA keith.obstein@vanderbilt.edu

Digital Object Identifier (DOI): see top of this page.

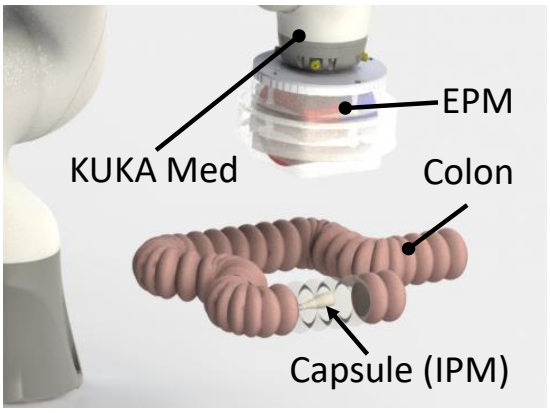

Figure 1. Schematic representation of the platform.

reduce discomfort for the patient and risk of adverse events.

This paper is organized as follows: in Section II we provide a general overview of the method, which is utilised and explored further in Section III. Sections IV and V present the experimental results, comparing the proposed approach with the ones discussed in [24], [20]; the former discusses free space levitation in a L-shaped acrylic tube, the latter reports the results obtained in a more realistic environment (a colon phantom). In Appendix A, we discuss the basic concepts of the magnetic actuation, while Appendix B reports proofs of lemmas and theorems employed in the paper.

II. Control Overview

The dynamic control approach discussed in the following is achieved using a single EPM controlled by a serial manipulator. Another magnet, referred to as IPM[1] is housed within the capsule. This is shown in Fig. 1.

In this scenario, the most unstable equilibrium is the one along the gravity direction. In fact, we need to guarantee that the force on the IPM counteracts gravity in an equilibrium state that is highly unstable. A dynamic control approach takes into account all forces that act on the system. In particular, the coupling between magnets is directly expressed in terms of interaction (generalized) forces; levitation is the outcome of the equilibrium of these forces with gravity.

In our previous work [20], we proposed a dynamic control approach that allows the IPM to levitate in a realistic environment, such as a colon phantom. The main drawback of this technique lies in two main assumptions: the desired trajectory was considered as a *piece-wise constant function of the time* and IPM-tether interactions were assumed negligible. The former restricts velocity of the IPM movements, while the latter does not guarantee convergence in a general scenario. In this paper, we aim to weaken both assumptions by employing an *adaptive dynamic* control and by proving *ultimately uniform bounded stability* of the proposed approach.

Compared to the previously proposed solution [20], we present a novel approach which takes into consideration the dynamics of IPM and deals with possible parametric uncertainties. The proposed technique is an *adaptive* control, which considers uncertainties such as the mass, dimensions of the IPM and the dynamics of the tether. In particular, the IPM mass is strongly affected by the tether. In fact, during levitation, a consistent section of the tether is lifted. The proposed control strategy autonomously modifies its parameters in order to adapt them to the actual system dynamics. Therefore, a further control loop has been inserted in the dynamic control in order to achieve convergence of the estimated dynamic parameters.

[1]In the following the soft-tethered capsule is also referred to as Internal Permanent Magnet.

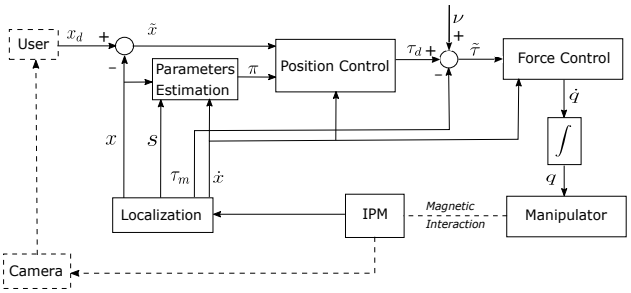

Figure 2. Control scheme.

III. Dynamic Control

The control strategy proposed herein is based on the *backstepping technique* which, compared to [24], [4], adds a control loop on the force. This improves controller stability, as discussed in [20]. Moreover, as an advancement of [20], we added a further internal loop which estimates the dynamics of the IPM and takes into account the effect of the tether. The scheme in Fig. 2 shows the proposed control strategy (solid lines). The external loop (dashed lines) represents the user interface which is not investigated in the present work.

Therefore, the control has three key components: pose control (Section III-A), parameters estimation (Section III-B) and force control (Section III-C). Pose control, considered as the external loop, aims to steer the IPM to the desired pose. The parameter estimation improves the controller properties, since this allows the assumptions to be weakened by the knowledge of the system dynamics. Force control, referred to also as "internal loop", aims to converge the actual force to the desired one. The stability of this backstepping approach, as shown in Section III-D, guarantees the overall convergence.

Fundamentally, the dynamics of the IPM is subjected to the magnetic interaction between EPM and IPM. The magnetic fields are approximated by the *dipole model* and are considered accurate for our purpose: given the geometry and relative distance between the two magnets, we can infer that the error does not significantly affect the control of the IPM. Possible errors related to dipole modelling are discussed in Section IV. The magnetic force and torque, exerted by the EPM on the IPM, can be written as a vector $\tau_m(x, q) \in \mathbb{R}^n$.

Consider the nominal dynamics of the IPM

$$B(x)\ddot{x} + C(x, \dot{x})\dot{x} + G(x) = \tau_m(x, q), \tag{1}$$

where $x \in \mathbb{R}^n$ is the IPM pose (i.e. position and orientation) and $q \in \mathbb{R}^m$ embeds the robot joint variables; $B(x)$, $C(x,\dot{x})$, $G(x)$ are referred to as *inertia*, *Coriolis matrix* and *gravity* [25] of the IPM, respectively. Our aim is to find q such that x approaches a desired value x_d.

This is achieved in two steps: first the value of the desired torque (τ_d) is found for $x \to x_d$, considering the dynamics of the unknown parameters, then we define $\dot{q}$ for which $\tau_m \to \tau_d$, according to the dynamics of the force and torque

$$\dot{\tau}_m = \frac{\partial \tau(x,q)}{\partial x}\dot{x} + \frac{\partial \tau(x,q)}{\partial q}\dot{q} = J_x\dot{x} + J_q\dot{q}. \tag{2}$$

The analytical computation of the matrices J_x and J_q is thoroughly explained in Appendix I. The variables $\dot{q}$ can be integrated to control the robot through its Direct Kinematics (DK) [25]. The novelty of our control system, compared to [24], is that we apply a closed-loop control on τ_m, as in [20]. Compared to [20], we introduced a further control loop in which we guarantee the convergence of the unknown parameters of the dynamic system.

The proposed approach takes into consideration how the tether can affect the dynamics of the IPM. It is herein considered an unmodelled disturbance on the IPM dynamics, in order to underline the robustness of the proposed approach. However, we show the stability of the proposed technique (Theorem 1) also in absence of the tether, as in the case of untethered capsules [4]. We do not consider the case of known tether properties since, even in the case tether dynamics can be predicted, interaction with the environment would confound them. Therefore, we consider the most general case of dynamic control of a single IPM.

In order to consider possible parametric uncertainties, embedded in the parameters vector $\pi \in \mathbb{R}^p$, we rewrite the dynamics in (1) as

$$B(x)\ddot{x} + C(x,\dot{x})\dot{x} + G(x) = Y(x,\dot{x},\ddot{x})\pi, \tag{3}$$

where $Y(x,\dot{x},\ddot{x}) \in R^{n\times p}$ is the *dynamic regressor*, computed as in [26]. The update law of π allows the unknown parameters to converge to their real values, guaranteeing the robust asymptotic stability of the overall system. Appendix B describes this in more detail.

The overall dynamics of the system we aim to control reads as

$$\begin{cases} Y(x,\dot{x},\ddot{x})\pi &= \tau \\ \dot{\tau} &= J_x\dot{x} + J_q\dot{q} + \dot{\nu} \end{cases}, \tag{4}$$

where ν models the tether interaction with the environment (such as: drag, elastic behaviour, friction and colon motions) and π embeds the uncertain parameters of the IPM, such as the mass, the length and the diameter. The localization method [22] measures x and $\dot{x}$, while the robot joints are measured by the embedded encoders.

A. Pose Control

As a first step, we define a pose controller that attempts to steer the IPM to a desired trajectory x_d. We aim to find a set of desired forces and torques, referred to as τ_d, that steer the IPM to the desired pose. Compared to [20], we consider partial knowledge of the dynamics of the system, using the *Adaptive Backstepping Control* [21], [27].

The control law can be determined directly through a standard Lyapunov approach, by defining

$$\begin{aligned} \tau_d &= \hat{B}(x)\ddot{x}_r + \hat{C}(x,\dot{x})\dot{x}_r + \hat{G}(x) - K_d s - \tilde{x} \\ &= Y(x,\dot{x},\dot{x}_r,\ddot{x}_r)\hat{\pi} - K_d s - \tilde{x} \end{aligned} \tag{5}$$

where $\hat{B}$, $\hat{C}$ and $\hat{C}$ are the estimated dynamic matrices, whose parameters are embedded in $\hat{\pi}$. The position error of the IPM is defined as $\tilde{x} = x_d - x$ and $s = \dot{\tilde{x}} + \Lambda\tilde{x} = \dot{x} - (\dot{x}_d - \Lambda\tilde{x}) = \dot{x} - \dot{x}_r$, with Λ symmetric, positive definite design matrix; $\dot{x}_r$ is referred to as the *reference velocity*, being the velocity the IPM is controlled to.

The present control loop guarantees $x \to x_d$, as $\tau \to \tau_d$. This statement holds under the following assumption.

Assumption 1: The steering of the IPM is achieved under these conditions:

- the force control, described in Section III-C, is faster than the system dynamics in (1);
- the unknown parameters vector π in (3) is constant.

The former leads to consider almost instantaneous convergence of force and torque; in fact, we assume there exists an instant T, $0 < T \ll 1$, such that $\tau(t) = \tau_d(t)$, for any $t \geq T$. This assumption is needed to prove Lemma 1 on which the final proof of this work (Theorem 1) is based. Furthermore, the need for $\pi = \text{const}$ is not limiting, since the inertial, Coriolis and gravity parameters do not generally vary over time.

Lemma 1: Under Assumption 1, the pose controller in (5) achieves asymptotic stability of the error $\tilde{x}$, for any positive definite design gains K_d and Λ.
Appendix B includes further details on this.

B. Parameters Estimation

This internal loop estimates the unknown parameters of the IPM dynamics, such as the mass and the dimensions of the IPM; this allows us to adapt our controller to the real dynamics of the system.

The control law is derived from the Lyapunov theory, defining $\dot{\tilde{\pi}} = \dot{\pi} - \dot{\hat{\pi}} = -\dot{\hat{\pi}} = u_\pi$, under the assumption that the unknown parameters vector π is constant. The control law reads as

$$u_\pi = R^{-1}Y^T(x,\dot{x},\dot{x}_r,\ddot{x}_r)s \tag{6}$$

where R is a positive, definite designed gain. The choice for u_π is justified by the proof of Lemma 1, reported in Appendix B.

C. Force Control

As the third step, we design a controller that ensures the magnetic force (τ_m) converges on the desired force (τ_d). According to Assumption 1, this loop is required to converge almost instantaneously. The magnetic force and torque are computed from x and q by employing the localization output and dipole model.

According to (2), the choice for

$$\dot{q} = J_q^{\dagger}(\dot{\tau}_d + K\tilde{\tau} - J_x\dot{x}). \tag{7}$$

yields to

$$\dot{\tilde{\tau}} = \dot{\tau}_d - \dot{\tau}_m = -K\tilde{\tau}, \tag{8}$$

with K positive definite design gain [20]. This leads to asymptotic stability of the force and torque error dynamics.

Lemma 2 (from [20]*):* Any choice for the positive definite gain K achieves stability of the torque dynamics, if $\nu = 0$.

D. Overall Control

In the following, we describe the overall control strategy by considering the previous sections. We show that the new choice of $\dot{q}$

$$\begin{cases} \tau_d &= Y(x, \dot{x}, \dot{x}_r, \ddot{x}_r)\hat{\pi} - K_d s - \tilde{x} \\ \dot{q} &= J_q^{\dagger}(\dot{\tau}_d + K\tilde{\tau} - J_x\dot{x} - \dot{x}) \\ u_\pi &= R^{-1}Y^T s \end{cases}, \tag{9}$$

leads to

$$\dot{\tilde{\tau}} = -K\tilde{\tau} + \dot{x},$$

which achieves overall convergence. This is is discussed in the following theorem.

Theorem 1: Under the assumption $\pi = \text{const}$, the controller defined in (9) attains, for any positive definite design gains K_p, K_d and K,

(a) asymptotic stability of $\tilde{x}$ if $\nu \simeq 0$;
(b) ultimately uniformly bounded error $\tilde{x}$ if ν is *piece-wise constant*.

This is discussed in Appendix B, where we underline that, even in the presence of unknown unmodelled disturbances related to the tether dynamics, stability of the error is ensured. Moreover, in the absence of disturbances (e.g. untethered IPMs), asymptotic stability is guaranteed.

IV. Experimental Analysis: Free Space Levitation

The goal of this experimental work is to validate the control strategy and show that IPM height (i.e. levitation) can be controlled and compare its performance with the two previous control strategies mentioned in this paper [24], [20].

The IPM is a cylindrical permanent magnet with an axial magnetization of 1.48 T (N52), diameter and length of 10.16 mm and a mass of 15 g. The EPM is a permanent magnet with a diameter and length of 101.6 mm and an axial magnetization of 1.48 T (N52). The EPM is attached to the flange of a serial manipulator (KUKA LBR Med robot[2]).

Table I reports the errors related to the dipole model, considering the mean distance between the two magnets during the experiments, described in [28].

To show how our control performs, we chose to navigate the IPM through an acrylic tube (Fig. 3) with an inner diameter of 60 mm and a 90 degrees bend in the middle. Each half of the tube has a length of 250 mm and the first part is inclined by approximately 20 mm over its length. In this case, the desired trajectory is a pre-planned path since we aim to objectively evaluate the levitating performance, without the user in the loop.

[2]https://www.kuka.com/en-de/industries/healthcare/kuka-medical-robotics

Table I
Mean error of the dipole model.

	Adaptive Backstepping	**Gravity compensating PD**	**PD**
EPM	3%	3.04%	2.5%
IPM	28.08%	27.8%	23.05%

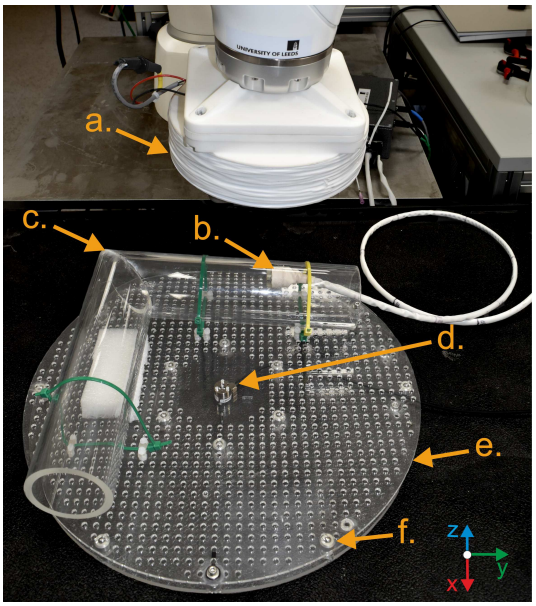

Figure 3. Sensorised platform. a. EPM, b. IPM, c. Environment (acrylic tube), d. Force/Torque sensor, e. Top acrylic sheet (constrained in negative z) and f. One of the ball transfer units

We compared this control approach with the techniques proposed in [20] and [24]. The latter imposes a continuous force along the gravity direction to maintain the magnetic coupling between the two magnets and therefore, imposes continuous contact with the environment; the former is able to levitate the IPM, but with limited velocity, due to the drawn assumptions. We performed 5 trials inside the tube with each method. A video of the experiments is reported in the attached media of the paper.

During the tests, we controlled the IPM to stay in the center of the lumen on the $x-y$ plane and to maintain levitation on the z axis. In the first tract of the tube, the main challenge for the controller is levitating the IPM, while in the second half of the tube, the stiffness of the tether and tube causes the IPM to maintain contact with the wall of the tube. However, the experiments show that the current control technique and the technique used in [20] are both able to resume IPM levitation after the disruption of moving past the corner.

To give a quantitative indication of the IPM's contact with the environment and, crucially, be able to compare the three control strategies, a custom sensorised force platform (Fig. 3) was used. The force sensor (6 axis Force/Torque sensor, Nano17, ATI) was secured between two acrylic sheets, with the top sheet constrained in the negative z direction but allowed

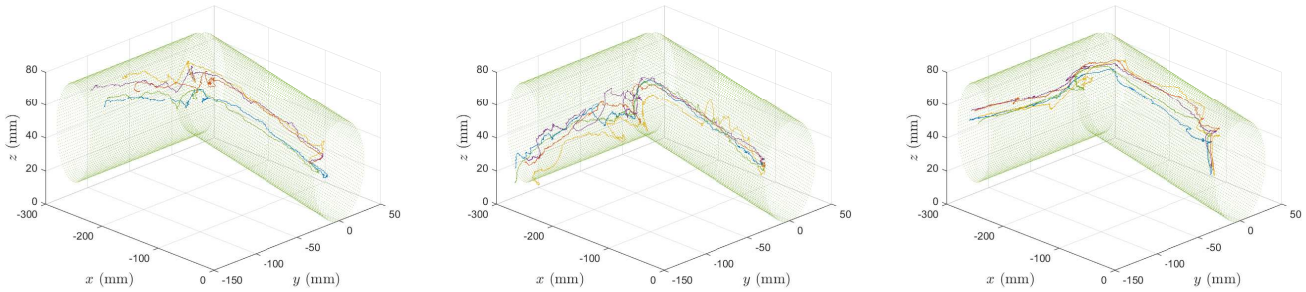

(a) Adaptive backstepping control. (b) Gravity compensating PD control [20]. (c) PD control [24].

Figure 4. 3D tracking.

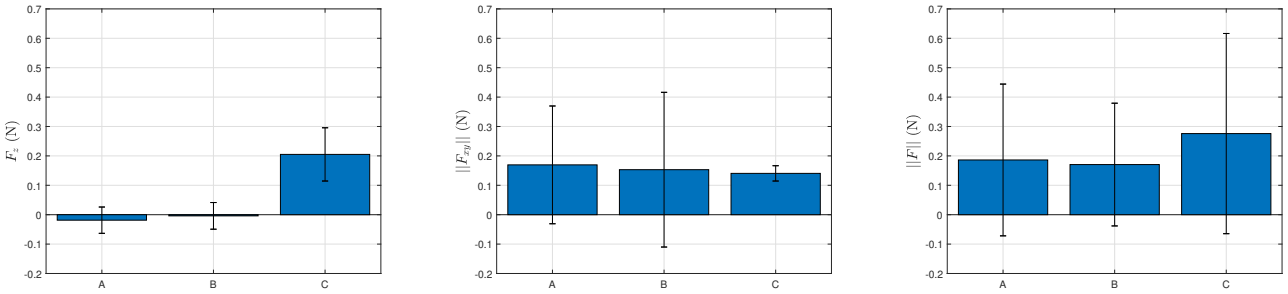

(a) Force along the z direction. (b) Norm of the lateral forces. (c) Overall IPM-tube contact.

Figure 5. Overview of the IPM-tube contact. A. Adaptive backstepping control. B. Gravity compensating PD control. C. PD control.

to move freely in x, y and positive z due to the ball transfer units used to support it. The sensor was used to precisely record (via a National Instruments cDAQ 9171, 1kHz sampling frequency) all forces acting on the acrylic sheet through the environment (i.e. acrylic tube). This setup was chosen to allow flexibility in the tube layout and the use of an extremely precise sensor (resolving down to approximately 0.003N) that could be damaged if connected to an unconstrained platform.

In Fig. 4, we report the 3D trajectories of the IPM for each approach, while in Fig. 5 we report the force on the z direction (gravity direction), the norm of the lateral force (along x and y axis) and the overall contact between the IPM and the tube wall, expressed as norm of the force vector.

The results show that the amount of contact with the current method is comparable to the results obtained with the gravity compensating PD approach, but is reduced with respect to the amount of contact achieved with the PD method. In fact, the force along the gravity direction is significantly lower with the first two approaches. Fig. 5(a) shows a negative mean value for the force with the Adaptive backstepping control and the Gravity compensating PD control. This is due to the force transmitted by the tether on the negative z axis. In general, we can infer that the IPM does not have contact with the tube wall; the limited contact with the tube is indicated from the standard deviation.

Moreover, due to the stiffness of the acrylic tube and the interaction of the tether, the norm of the overall force (i.e. taking into account force in the x and y direction) is significantly larger than the force in the z direction with the Adaptive Backstepping control and the Gravity compensating PD control approaches. This also underlines the robustness of the proposed approach towards significant interaction between the tether and the environment. On-the-other-hand, this issue is likely to be less significant in a more flexible environment, such as the colon. Therefore, the method is expected to attain a more satisfactory performance.

Moreover, in Fig. 4 we can notice that, with respect to the Gravity compensating PD control, the Adaptive backstepping control is able to maintain a better levitation also after the corner (where the rigidity of the tube and the stiffness of the tether affect the behaviour of the IPM). The gravity compensating PD control, instead, has more difficulty to exert necessary force to levitate the IPM while trying to reduce the IPM-tube contact.

Concerning the time to travel the tube and to resume the IPM levitation after the corner, we can infer that the Adaptive Backstepping control is faster than the gravity compensating PD method: with the Adaptive Backstepping control the IPM was able to traverse the tube in a mean time of 72 s with a standard deviation of 9.1 s, while the PD controller reports a mean time of 126.2 s with standard deviation of 23 s.

V. Experimental Analysis: Colon Phantom

To show the practical feasibility of this approach we provide experiments in a more realistic environment. For this purpose, we used the M40 Colonoscope Training Simulator[3] in *standard configuration*. As the previous set of the experiments

[3]https://www.kyotokagaku.com/products/detail01/m40.html

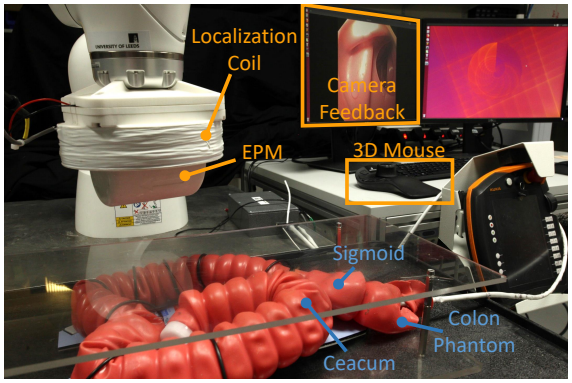

Figure 6. Setup for colon phantom experiments.

in Section IV, we compared the current approach with the method used in [20] and the PD control computed in [24].

We performed 5 trials with each approach to compare all techniques. The user (with no prior endoscopic experience, but knowledge of the platform) was able to guide the IPM to traverse the colon from the end of the sigmoid to the caecum. The IPM is equipped with a camera that provides a visual feedback to the user, which manipulates the IPM's desired pose (x_d) with a 3D mouse, as shown in Fig. 6.

In Fig. 7, we report the fastest trial with each approach. These experiments show that the current approach is able to reduce the mean completion time for the overall task (a path of approximately 0.85 m). The Adaptive Backstepping control achieves a mean completion time of 248.5 s with standard deviation of 31.8 s; the mean time achieved by the gravity compensating PD control [20] was 306.3 s with a standard deviation of 69.6 s; the PD control [24], instead, had a mean completion time of 551.9 s with standard deviation of 138.4 s. Moreover, since we set a maximum time for each trial of 600 s, the PD control failed two times over all five trials - the ceacum was not reached on time.

In order to levitate the capsule, the force exerted on the IPM along the z axis is reduced, compared to [24]; this leads to a lower functional steering force and the need for feeding the tether (i.e. assistance with overcoming tether drag). However, since the capsule is levitating, the friction related to environmental interaction is reduced and feeding the tether is more effective. A video of the experiment performed with the Adaptive backstepping control is reported in the attached media of the paper.

During these experiments, the sensorised platform was not used to measure the force that the IPM exerts on the environment. This was because the transmitted forces (from the IPM interactions to the sensor) were sufficiently low to be comparable with background noise. The attributing factor being the highly deformable environment that absorbs (dissipates) the low (<1N) contact forces. In the future, to investigate the real performance of the proposed approach, a deeper analysis will be performed with expert users.

A supplementary video shows the robustness of the control technique in the presence of external disturbances.

VI. Conclusion

The present paper discusses a dynamic approach for the control of the magnetically actuated medical robots. In particular, we show the application of the proposed technique to the MFE [1]. We prove that proposed method is enough accurate to achieve levitation of the IPM, which is one of the most complex tasks with this type of platforms. Moreover, levitating the IPM leads to reduced contact with the environment, avoiding obstacles and folds. This can aid locomotion and reduce tissue stress (i.e. patient discomfort and risk of trauma).

The control strategy is based on the *Adaptive Backstepping Control*, which facilitates IPM levitation. The novelty of the current approach is the fact that we take into account the dynamics of the IPM, considering all the uncertainties the system is subjected to. This overcomes some of the assumptions drawn in [20]. In particular, the assumption that the desired trajectory is a *piece-wise constant function of the time* is weakened. This allows an increase in the velocity of the IPM, even if this is always subjected to the limitation of the IPM localization algorithm. In fact, the current localization frequency (100 Hz) is not fast enough to guarantee that the IPM dynamics is handled completely and so increasing this would have a direct impact on system performance.

To prove the strength of the current approach we performed two sets of experiments. The first set of experiments was developed in free space, using a sensorised platform to measure the forces the IPM exerted on the environment. The measured force can be read as a measure of the amount of contact between the IPM and the tube wall. The results demonstrate that our method is able to reduce the contact with the surrounding and increase the velocity of the IPM respect to the previous solutions [20], [24].

To prove the feasibility of our approach in a more realistic environment, we performed the second set of experiments in a colon phantom. These proved that with the current strategy the IPM was able to traverse the colon from the sigmoid to the caecum with a reasonable completion time. Prior work using a latex phantom and Olympus colonoscope demonstrates a median cecal intubation time (i.e. travelling from anus to cecum) of 150.19 s (115.68, 197.48) for 4 experted physicians [29]. Even if the proposed method is slower compared to the standard technique, it is worth mentioning that the lower invasiveness of the MFE has the potential for eliminating the need for anesthesia and so achieve an overall shorter procedure and recovery time.

In the future, we will investigate the performance of the current approach in a more realistic experimental setting (i.e animal and cadaver models). Moreover, we aim to investigate the application of the proposed control approach to multiple IPMs.

Appendix A
Magnetic Actuation

Consider the vector between End Effector (EE) position (p_E) and IPM position (p_I), referred to as $p = p_E - p_I$.

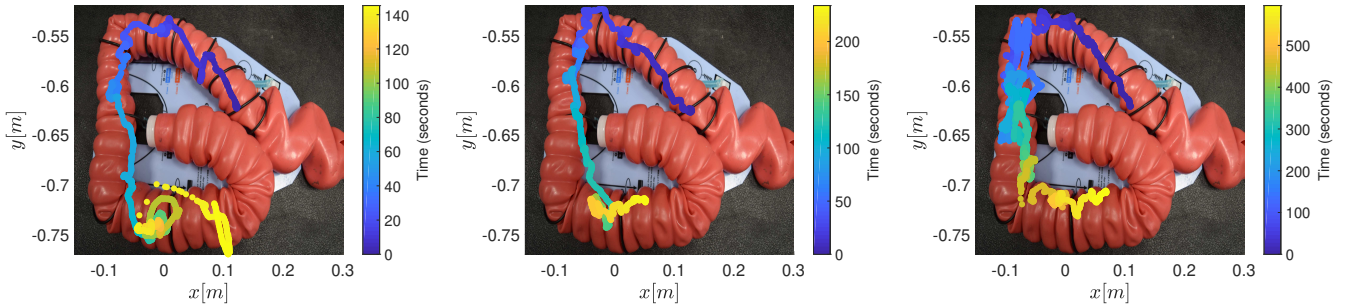

(a) Adaptive backstepping control. (b) Gravity compensating PD control [20]. (c) PD control [24].

Figure 7. Trials on the colon simulator.

According to the dipole model, the (generalized) force between EPM and IPM is

$$\tau_m = \begin{pmatrix} \frac{3M}{||p||^4}(\hat{m}_E\hat{m}_I^T + \hat{m}_I\hat{m}_E^T + (\hat{m}_I^T Z \hat{m}_E)I)\hat{p} \\ \frac{M}{||p||^3}\hat{m}_I \times D\hat{m}_E \end{pmatrix}$$

where $M = \frac{\mu_0 ||m_I||\ ||m_E||}{4\pi}$ with $m_I = ||m_I||\hat{m}_I$ and $m_E = ||m_E||\hat{m}_E$ *magnetic moments* of IPM and EPM, respectively; $\mu_0 = 4\pi 10^{-7}\frac{N}{A^2}$ permeability of vacuum, $\hat{p} = \frac{p}{||p||}$, $Z = I - 5\hat{p}\hat{p}^T$ and $D = 3\hat{p}\hat{p}^T - I$. Herein $I \in \mathbb{R}^{3\times 3}$ is referred to as the *identity matrix* and $||\cdot||$ is the *Euclidean norm*.

We consider the time derivative of τ_m [20]

$$\begin{aligned}\dot{\tau}_m &= \begin{pmatrix} \frac{\partial \tau_m}{\partial p} & \frac{\partial \tau_m}{\partial \hat{m}_E} \end{pmatrix} \begin{pmatrix} \dot{p}_E \\ \dot{\hat{m}}_E \end{pmatrix} - \begin{pmatrix} \frac{\partial \tau_m}{\partial p} & \frac{\partial \tau_m}{\partial \hat{m}_I} \end{pmatrix} \begin{pmatrix} \dot{p}_I \\ \dot{\hat{m}}_I \end{pmatrix} \\ &= \begin{pmatrix} \frac{\partial \tau_m}{\partial p} & \frac{\partial \tau_m}{\partial \hat{m}_E} \end{pmatrix} \begin{pmatrix} I & 0_{3,3} \\ 0_{3,3} & (\hat{m}_E)_\times^T \end{pmatrix} J\dot{q} \\ &\quad - \begin{pmatrix} \frac{\partial \tau_m}{\partial p} & \frac{\partial \tau_m}{\partial \hat{m}_I} \end{pmatrix} \begin{pmatrix} I & 0_{3,3} \\ 0_{3,3} & (\hat{m}_I)_\times^T \end{pmatrix} \dot{x} \\ &= J_q\dot{q} + J_x\dot{x},\end{aligned}$$

with J manipulator's Jacobian matrix.

APPENDIX B
PROOFS OF LEMMAS AND THEOREMS

In the following we provide the proofs of Lemma 1 and Theorem 1.

Proof of Lemma 1: Consider the positive definite Lyapunov function

$$W(\tilde{x}, s, \tilde{\pi}, t) = \frac{1}{2}\tilde{x}^T\tilde{x} + \frac{1}{2}s^T B(x)s + \frac{1}{2}\tilde{\pi}^T R\tilde{\pi}.$$

with R is a positive definite gain. Since the unknown parameters are assumed constant, their error dynamics is $\dot{\tilde{\pi}} = \dot{\pi} - \dot{\hat{\pi}} = -\dot{\hat{\pi}} \stackrel{\text{def}}{=} -u_\pi$, for some choice for the update law u_π. The time derivative of the chosen Lyapunov function reads as

$$\begin{aligned}\dot{W} &= \tilde{x}^T\dot{\tilde{x}} + s^T B(x)\dot{s} + \frac{1}{2}s^T\dot{B}(x)s - \tilde{\pi}^T R u_\pi \\ &= \tilde{x}^T\dot{\tilde{x}} + s^T(B(x)\ddot{x} - B(x)\ddot{x}_r) + \frac{1}{2}s^T\dot{B}(x)s - \tilde{\pi}^T R u_\pi\end{aligned}$$

Summing and subtracting $s^T C s$ we obtain

$$\begin{aligned}\dot{W} = \tilde{x}^T\dot{\tilde{x}} + s^T(-B(x)\ddot{x}_r - C(x,\dot{x})\dot{x}_r - G(x) + \tau) + \\ + \frac{1}{2}s^T(\dot{B}(x) - 2C(x,\dot{x}))s - \tilde{\pi}^T R u_\pi.\end{aligned}$$

Due to the *skew-symmetry* of $\dot{B}(x) - 2C(x,\dot{x})$, $\dot{s}^T(\dot{B}(x) - 2C(x,\dot{x}))\dot{s} = 0$ [25]. We define the generalized forces as

$$\tau = \hat{B}(x)\ddot{x}_r + \hat{C}(x,\dot{x})\dot{x}_r + \hat{G}(x) - K_d s - \tilde{x}.$$

thus

$$\dot{W} = s^T Y\tilde{\pi} - s^T K_d s - \tilde{x}^T\Lambda\tilde{x} - \tilde{\pi}^T R u_\pi.$$

The update law $u_\pi = R^{-1}Y^T s$, for the parameters dynamics, yields to

$$\dot{W} = -s^T K_d s - \tilde{x}^T\Lambda\tilde{x}$$

and leads to conclude for, at least, *uniform stability* of the origin.

According to La Salle-Yoshizawa's theorem [30], since $\lim_{t\to\infty}\dot{W}(\tilde{x}, s, \tilde{\pi}) = 0$, $\lim_{t\to\infty}\tilde{x} = 0$ and asymptotic stability of $\tilde{x}$ is guaranteed.

Proof of Theorem 1: Consider the positive definite Lyapunov function

$$V(\tilde{x}, s, \tilde{\pi}, t, \tilde{\tau}) = W(\tilde{x}, s, \tilde{\pi}, t) + \frac{1}{2}\overline{\tau}^T\overline{\tau},$$

where $W(\tilde{x}, s, \tilde{\pi}, t)$ is the Lyapunov function defined in the proof of Lemma 1 and $\overline{\tau} = \tau_d - \tau$. The time derivative of the chosen Lyapunov function is

$$\begin{aligned}\dot{V}(\tilde{x}, s, \tilde{\pi}, t, \tilde{\tau}) &= -s^T K_d s - \tilde{x}^T\Lambda\tilde{x} + (\tilde{\tau} + \nu)^T\dot{\tilde{\tau}} \\ &= -s^T K_d s - \tilde{x}^T\Lambda\tilde{x} - \tilde{\tau}^T K\tilde{\tau} - \nu^T K\tilde{\tau},\end{aligned}$$

under the assumption $\dot{\nu} \simeq 0$.

First, we prove statement (a). In absence of disturbances, i.e. $\nu = 0$, by applying the La Salle-Yoshizawa's theorem [30], we can conclude for asymptotic stability of $\tilde{x}$, as in the proof of Lemma 1.

We can also investigate the uniform ultimate boundedness of $\tilde{x}$ (statement (b)), by showing that for any $0 < \theta < 1$,

$$\begin{aligned}\dot{V}(\tilde{x}, s, \tilde{\pi}, t, \tilde{\tau}) = (1-\theta)(-s^T K_d s - \tilde{x}^T\Lambda\tilde{x} - \tilde{\tau}^T K\tilde{\tau}) + \\ \theta(-s^T K_d s - \tilde{x}^T\Lambda\tilde{x} - \tilde{\tau}^T K\tilde{\tau}) - \dot{\nu}^T K\tilde{\tau},\end{aligned}$$

therefore,

$$\dot{V}(\tilde{x}, s, \tilde{\pi}, t, \tilde{\tau}) \leq \overline{\lambda}(K_d, \Lambda, K)||\tilde{\xi}|| \quad \forall\ 0 < \theta < 1,$$

if

$$||\tilde{\xi}|| = \frac{-\overline{\lambda}(K)||\dot{\nu}||}{\theta\overline{\lambda}(K_d, \Lambda, K)} \stackrel{\text{def}}{=} \mu.$$

Here $\tilde{\xi} = (s^T \ \tilde{x}^T \ \tilde{\tau}^T)^T$ and $\overline{\lambda}(A_1, A_2, \ldots, A_l)$ is referred as the maximum eigenvalue of the matrices $A_1, A_2, \ldots, A_l$.

Therefore, the ultimate bound is μ.

REFERENCES

[1] A. Arezzo, A. Menciassi, P. Valdastri, G. Ciuti, G. Lucarini, M. Salerno, C. Di Natali, M. Verra, P. Dario, and M. Morino, "Experimental assessment of a novel robotically-driven endoscopic capsule compared to traditional colonoscopy," *Digestive and Liver Disease*, vol. 45, no. 8, pp. 657–662, 2013. [Online]. Available: http://dx.doi.org/10.1016/j.dld.2013.01.025

[2] P. Valdastri, C. Quaglia, E. Susilo, A. Menciassi, P. Dario, C. Ho, G. Anhoeck, and M. Schurr, "Wireless therapeutic endoscopic capsule: in vivo experiment," *Endoscopy*, vol. 40, no. 12, pp. 979–982, dec 2008. [Online]. Available: http://www.thieme-connect.de/DOI/DOI?10.1055/s-0028-1103424

[3] P. Valdastri, G. Ciuti, A. Verbeni, A. Menciassi, P. Dario, A. Arezzo, and M. Morino, "Magnetic air capsule robotic system: proof of concept of a novel approach for painless colonoscopy," *Surgical Endoscopy*, vol. 26, no. 5, pp. 1238–1246, 2012. [Online]. Available: https://doi.org/10.1007/s00464-011-2054-x

[4] A. W. Mahoney and J. J. Abbott, "Five-degree-of-freedom manipulation of an untethered magnetic device in fluid using a single permanent magnet with application in stomach capsule endoscopy," *The International Journal of Robotics Research*, vol. 35, no. 1-3, pp. 129–147, 2016.

[5] C. Chautems and B. J. Nelson, "The tethered magnet: Force and 5-DOF pose control for cardiac ablation," *Proceedings - IEEE International Conference on Robotics and Automation*, pp. 4837–4842, 2017.

[6] M. N. Faddis, W. Blume, J. Finney, A. Hall, J. Rauch, J. Sell, K. T. Bae, M. Talcott, and B. Lindsay, "Novel, magnetically guided catheter for endocardial mapping and radiofrequency catheter ablation," *Circulation*, vol. 106, no. 23, pp. 2980–2985, 2002.

[7] S. Toggweiler, J. Leipsic, R. K. Binder, M. Freeman, M. Barbanti, R. H. Heijmen, D. A. Wood, and J. G. Webb, "Management of vascular access in transcatheter aortic valve replacement: Part 2: Vascular complications," *JACC: Cardiovascular Interventions*, vol. 6, no. 8, pp. 767–776, 2013.

[8] S. K. Hilai, W. Jost Michelsen, J. Driller, and E. Leonard, "Magnetically guided devices for vascular exploration and treatment," *Radiology*, vol. 113, no. 3, pp. 529–540, 1974, pMID: 4428036. [Online]. Available: https://doi.org/10.1148/113.3.529

[9] S. Ernst, F. Ouyang, C. Linder, K. Hertting, F. Stahl, J. Chun, H. Hachiya, D. Bänsch, M. Antz, and K.-H. Kuck, "Initial experience with remote catheter ablation using a novel magnetic navigation system," *Circulation*, vol. 109, no. 12, pp. 1472–1475, 2004. [Online]. Available: https://www.ahajournals.org/doi/abs/10.1161/01.CIR.0000125126.83579.1B

[10] E. Diller, J. Giltinan, G. Z. Lum, Z. Ye, and M. Sitti, "Six-degree-of-freedom magnetic actuation for wireless microrobotics," *International Journal of Robotics Research*, vol. 35, no. 1-3, pp. 114–128, 2016.

[11] J. Edelmann, A. J. Petruska, and B. J. Nelson, "Estimation-Based Control of a Magnetic Endoscope without Device Localization," *Journal of Medical Robotics Research*, vol. 03, no. 01, p. 1850002, Mar 2018. [Online]. Available: http://www.worldscientific.com/doi/abs/10.1142/S2424905X18500022

[12] A. J. Petruska and B. J. Nelson, "Minimum Bounds on the Number of Electromagnets Required for Remote Magnetic Manipulation," *IEEE Transactions on Robotics*, vol. 31, no. 3, pp. 714–722, 2015.

[13] C. Chautems, A. Tonazzini, D. Floreano, and B. J. Nelson, "A variable stiffness catheter controlled with an external magnetic field," *2017 IEEE/RSJ International Conference on Intelligent Robots and Systems (IROS)*, pp. 181–186, 2017. [Online]. Available: http://ieeexplore.ieee.org/document/8202155/

[14] T. Greigarn, R. Jackson, T. Liu, and M. C. Çavuşoğlu, "Experimental validation of the pseudo-rigid-body model of the MRI-actuated catheter," in *2017 IEEE International Conference on Robotics and Automation (ICRA)*, May 2017, pp. 3600–3605.

[15] S. Jeon, A. K. Hoshiar, K. Kim, S. Lee, E. Kim, S. Lee, J. Kim, B. J. Nelson, H. Cha, B. Yi, and H. Choi, "A magnetically controlled soft microrobot steering a guidewire in a three-dimensional phantom vascular network," *Soft Robotics*, vol. 0, no. 0, 0, pMID: 30312145. [Online]. Available: https://doi.org/10.1089/soro.2018.0019

[16] J. Sikorski, I. Dawson, A. Denasi, E. E. Hekman, and S. Misra, "Introducing BigMag - A novel system for 3D magnetic actuation of flexible surgical manipulators," *Proceedings - IEEE International Conference on Robotics and Automation*, pp. 3594–3599, 2017.

[17] S. Yim and M. Sitti, "Design and Rolling Locomotion of a Magnetically Actuated Soft Capsule Endoscope," *IEEE Transactions on Robotics*, vol. 28, no. 1, pp. 183–194, Feb 2012.

[18] P. Ryan and E. Diller, "Magnetic Actuation for Full Dexterity Microrobotic Control Using Rotating Permanent Magnets," *IEEE Transactions on Robotics*, vol. 33, no. 6, pp. 1398–1409, 2017.

[19] C. Tremblay, B. Conan, D. Loghin, A. Bigot, and S. Martel, "Fringe field navigation for catheterization," in *6th European Conference of the International Federation for Medical and Biological Engineering*, I. Lacković and D. Vasic, Eds. Cham: Springer International Publishing, 2015, pp. 379–382.

[20] G. Pittiglio, L. Barducci, J. W. Martin, J. Norton, C. A. Avizzano, K. Obstein, and P. Valdastri, "Magnetic levitation for soft-tethered capsule colonoscopy actuated with a single permanent magnet: a dynamic control approach," *IEEE Robotics and Automation Letters*, pp. 1–1, 2019.

[21] J. Zhou and C. Wen, *Adaptive backstepping control of uncertain systems: Nonsmooth nonlinearities, interactions or time-variations*. Springer, 2008.

[22] A. Z. Taddese, P. R. Slawinski, M. Pirotta, E. De Momi, K. L. Obstein, and P. Valdastri, "Enhanced real-time pose estimation for closed-loop robotic manipulation of magnetically actuated capsule endoscopes," *The International Journal of Robotics Research*, vol. 37, no. 8, pp. 890–911, 2018. [Online]. Available: https://doi.org/10.1177/0278364918779132

[23] M. Turan, J. Shabbir, H. Araujo, E. Konukoglu, and M. Sitti, "A deep learning based fusion of rgb camera information and magnetic localization information for endoscopic capsule robots," *International Journal of Intelligent Robotics and Applications*, vol. 1, no. 4, pp. 442–450, Dec 2017. [Online]. Available: https://doi.org/10.1007/s41315-017-0039-1

[24] A. Z. Taddese, P. R. Slawinski, K. L. Obstein, and P. Valdastri, "Nonholonomic closed-loop velocity control of a soft-tethered magnetic capsule endoscope," in *2016 IEEE/RSJ International Conference on Intelligent Robots and Systems (IROS)*. IEEE, Oct 2016, pp. 1139–1144. [Online]. Available: http://ieeexplore.ieee.org/document/7759192/

[25] B. Siciliano, L. Sciavicco, L. Villani, and G. Oriolo, *Robotics: Modelling, Planning and Control*, 1st ed. Springer Publishing Company, Incorporated, 2008.

[26] M. Gabiccini, A. Bracci, D. De Carli, M. Fredianelli, and A. Bicchi, "Explicit lagrangian formulation of the dynamic regressors for serial manipulators," in *Proceedings of the XIX Aimeta Congress*, 2009.

[27] H. K. Khalil, *Nonlinear systems*. Macmillan Pub. Co., 1992. [Online]. Available: https://books.google.co.uk/books?id=RVHvAAAAMAAJ

[28] A. J. Petruska and J. J. Abbott, "Optimal permanent-magnet geometries for dipole field approximation," *IEEE Transactions on Magnetics*, vol. 49, no. 2, pp. 811–819, Feb 2013.

[29] K. L. Obstein, V. D. Patil, J. Jayender, R. S. J. Estpar, I. S. Spofford, B. I. Lengyel, K. G. Vosburgh, and C. C. Thompson, "Evaluation of colonoscopy technical skill levels by use of an objective kinematic-based system," *Gastrointestinal Endoscopy*, vol. 73, no. 2, pp. 315–321.e1, 2011. [Online]. Available: http://dx.doi.org/10.1016/j.gie.2010.09.005

[30] J. T. Spooner, M. Maggiore, R. Ordonez, and K. M. Passino, *Stable Adaptive Control and Estimation for Nonlinear Systems- Neural and Fuzzy Approximator Techniques*. John Wiley & Sons, 2002.